

A Clinical Metabolite of Azidothymidine Inhibits Experimental Choroidal Neovascularization and Retinal Pigmented Epithelium Degeneration

Siddharth Narendran,¹⁻³ Felipe Pereira,^{1,2} Praveen Yerramothu,^{1,2} Ivana Apicella,^{1,2} Shao-bin Wang,^{1,2} Akhil Varshney,^{1,2} Kirstie L. Baker,⁴ Kenneth M. Marion,⁴ Meenakshi Ambati,^{1,2,5} Vidya L. Ambati,⁵ Kameshwari Ambati,^{1,2} Srinivas R. Sadda,^{4,6} Bradley D. Gelfand,^{1,2,7} and Jayakrishna Ambati^{1,2,8-10}

¹Center for Advanced Vision Science, University of Virginia School of Medicine, Charlottesville, Virginia, United States

²Department of Ophthalmology, University of Virginia School of Medicine, Charlottesville, Virginia, United States

³Aravind Eye Care System, Madurai, India

⁴Doheny Eye Institute, Los Angeles, Los Angeles, California, United States

⁵Center for Digital Image Evaluation, Charlottesville, Virginia, United States

⁶Department of Ophthalmology, David Geffen School of Medicine, University of California-Los Angeles, Los Angeles, California, United States

⁷Department of Biomedical Engineering, University of Virginia School of Medicine, Charlottesville, Virginia, United States

⁸Department of Pathology, University of Virginia School of Medicine, Charlottesville, Virginia, United States

⁹Department of Neuroscience, University of Virginia School of Medicine, Charlottesville, Virginia, United States

¹⁰Department of Microbiology, Immunology, and Cancer Biology, University of Virginia School of Medicine, Charlottesville, Virginia, United States

Correspondence: Jayakrishna Ambati, Center for Advanced Vision Science, University of Virginia School of Medicine, 415 Lane Road, Charlottesville, VA 22908, USA; ja9qr@virginia.edu.

Received: May 14, 2020

Accepted: July 12, 2020

Published: August 4, 2020

Citation: Narendran S, Pereira F, Yerramothu P, et al. A clinical metabolite of azidothymidine inhibits experimental choroidal neovascularization and retinal pigmented epithelium degeneration. *Invest Ophthalmol Vis Sci.* 2020;61(10):4. <https://doi.org/10.1167/iovs.61.10.4>

PURPOSE. Azidothymidine (AZT), a nucleoside reverse transcriptase inhibitor, possesses anti-inflammatory and anti-angiogenic activity independent of its ability to inhibit reverse transcriptase. The aim of this study was to evaluate the efficacy of 5'-glucuronyl azidothymidine (GAZT), an antiretrovirally inert hepatic clinical metabolite of AZT, in mouse models of retinal pigment epithelium (RPE) degeneration and choroidal neovascularization (CNV), hallmark features of dry and wet age-related macular degeneration (AMD), respectively.

METHODS. RPE degeneration was induced in wild-type (WT) C57BL/6J mice by subretinal injection of *Alu* RNA. RPE degeneration was assessed by fundus photography and confocal microscopy of zonula occludens-1-stained RPE flat mounts. Choroidal neovascularization was induced by laser injury in WT mice, and CNV volume was measured by confocal microscopy. AZT and GAZT were delivered by intravitreal injections. Inflammation activation was monitored by western blotting for caspase-1 and by ELISA for IL-1 β in *Alu* RNA-treated bone marrow-derived macrophages (BMDMs).

RESULTS. GAZT inhibited *Alu* RNA-induced RPE degeneration and laser-induced CNV. GAZT also reduced *Alu* RNA-induced caspase-1 activation and IL-1 β release in BMDMs.

CONCLUSIONS. GAZT possesses dual anti-inflammatory and anti-angiogenic properties and could be a viable treatment option for both forms of AMD.

Keywords: macular degeneration, RPE degeneration, choroidal neovascularization

Age-related macular degeneration (AMD) is the predominant cause of blindness among the elderly in the industrially developed world.¹ AMD is classified into atrophic (non-neovascular) and neovascular forms. Although this dichotomization is convenient, recent studies have identified significant overlap in the pathophysiological mechanisms driving disease initiation and progression of these ostensibly distinct clinical entities.²⁻⁴ Despite these similarities, they differ considerably in terms of treatment options. Although effective treatment with anti-vascular endothelial growth factor (VEGF) is available for neovascular AMD, no approved therapy exists for the atrophic form. Despite

its efficacy in neovascular AMD, anti-VEGF therapy does not provide benefit for atrophic AMD.⁵ Therefore, a single therapy for both forms of AMD would be a welcome development.

Retinal pigment epithelium (RPE) degeneration and choroidal neovascularization (CNV) are the hallmark clinical features of atrophic and neovascular AMD, respectively.⁶ Azidothymidine (AZT), a nucleoside reverse transcriptase inhibitor (NRTI), possesses both anti-inflammatory and anti-angiogenic activities and has been shown to be effective in animal models of CNV and RPE degeneration.^{7,8} However, the systemic toxicity associated with AZT makes it less than

ideal as a repurposing drug candidate for AMD.⁹ This toxicity is associated directly with its ability to inhibit reverse transcriptase, an activity necessary for its anti-retroviral function but unessential for its anti-inflammatory activity.^{10–12} Hence, identification of AZT analogs that lack the ability to inhibit reverse transcriptase and assessing the anti-inflammatory and anti-angiogenic properties of these analogs may help identify potential drug candidates for AMD.

Following oral administration, AZT is rapidly absorbed and metabolized. The predominant metabolite of AZT in humans, 5'-glucuronyl azidothymidine (GAZT), accounts for ~70% of all excreted AZT and is inactive against retroviral replication.^{13,14} The aim of this study was to investigate if GAZT retains the anti-inflammatory and anti-angiogenic properties of AZT by assessing its efficacy in mouse models of geographic atrophy (GA) and CNV.

METHODS

Animals

Both male and female wild-type (WT) C57BL/6J mice between 6 and 10 weeks of age purchased from The Jackson Laboratory (Bar Harbor, ME, USA) were used in this study. For all procedures, anesthesia was achieved by intraperitoneal injection of 100 mg/kg ketamine hydrochloride (Fort Dodge Animal Health, Overland Park, KS, USA) and 10 mg/kg xylazine (Anased, Akorn, Decatur, IL, USA), and pupils were dilated with topical 1% tropicamide and 2.5% phenylephrine hydrochloride (Alcon, Fort Worth, TX, USA). All animal experiments were approved by the University of Virginia Institutional Animal Care and Use Committee and was performed in accordance with the ARVO Statement for the Use of Animals in Ophthalmic and Visual Research.

Subretinal Injections

Subretinal injections (1 μ L) of in vitro transcribed *Alu* RNA (300 ng/ μ L) were performed in mice using a 35-gauge needle (Ito Corporation, Tokyo, Japan) as previously described.¹⁵

Laser-Induced CNV

Experimental CNV was induced by performing laser photocoagulation with an OcuLight GL laser system (532 nm, 180 mW, 100 ms, 75 μ m; Iridex Corporation, Mountain View, CA, USA) bilaterally in 6- to 8-week-old mice by creating four laser lesions per eye.

Drug Treatments

Intravitreal administration of 0.5 nmol AZT (Selleck Chemicals, Houston, TX, USA), 0.25 to 2.5 nmol GAZT (Cayman Chemical, Ann Arbor, MI, USA), or vehicle (PBS) in a volume of 0.5 μ L was performed using an Ito 35-gauge needle immediately after subretinal injection or laser injury.

CNV Volume Measurement

At 1 week after the laser injury, eyes were enucleated and fixed with 4% paraformaldehyde for 30 minutes at 4°C. RPE flat mounts were obtained after the neurosensory retina was gently detached and severed from the optic nerve. The flat mounts were then washed in PBS, followed by

dehydration and rehydration through a methanol series. After blocking in PBS with 1% bovine serum albumin (Sigma-Aldrich, St. Louis, MO, USA) and 0.5% Triton X-100 (Sigma-Aldrich) for 1 hour at room temperature, flat mounts were incubated with 0.7% FITC-isolectin B4 (Vector Laboratories, Burlingame, CA, USA) overnight at 4°C. The RPE-choroid-sclera complex was then flat mounted in antifade medium (Immu-Mount Vectashield Mounting Medium; Vector Laboratories) and cover slipped. Choroidal neovascularization was visualized using a blue argon laser wavelength (488 nm) and a scanning laser confocal microscope (A1R confocal microscope system; Nikon, Tokyo, Japan), and quantified using FIJI software (<http://fiji.sc/>).

Fundus Photography

Fundus imaging of dilated mouse eyes was performed using a TRC-50 IX camera (Topcon, Tokyo, Japan) linked to a digital imaging system (Sony, Tokyo, Japan).

Assessment of RPE Degeneration

Seven days after subretinal injection, RPE health was assessed by fundus photography and immunofluorescence staining of zonula occludens-1 (ZO-1) on RPE flat mounts (whole mount of posterior eye cup containing RPE and choroidal layers). Mouse RPE and choroidal flat mounts were fixed with 2% paraformaldehyde, stained with rabbit polyclonal antibodies against mouse ZO-1 (1:100, Invitrogen, Carlsbad, CA, USA) and visualized with Alexa Fluor 594 (Invitrogen). All images were obtained by confocal microscopy (Nikon A1R confocal microscope system). Imaging was performed by an operator blinded to the group assignments.

RPE degeneration was quantified based on ZO-1-stained flat mount images using two strategies:

1. For the binary assignment approach, RPE health was assessed as the presence or absence of morphological disruption in RPE flat mounts by two independent raters who were masked to the group assignments.^{7,15–17} Both raters deemed 100% of the images as gradable (inter-rater agreement = 100%; Pearson $r^2 = 1$, $P < 0.0001$).
2. Semi-automated cellular morphometry analysis for hexagonally packed cells was performed by two masked graders as previously described.¹⁶ For this analysis, microscopy images of the RPE were captured and transmitted in a de-identified fashion to the Doheny Image Reading & Research Lab. All images were rescaled to 304 \times 446 pixels to permit importation into the Konan CellChek software (version 4.0.1), a commercial US Food and Drug Administration-cleared software that has been used for clinical trials. RPE cell metrics were generated by two certified reading center graders in an independent, masked fashion. When the cell centers had been defined, the software automatically generated the polymegathism (PM) values.

Cell Culture

All cells were maintained at 37°C in a 5% CO₂ environment. Bone marrow-derived macrophages (BMDMs) were isolated from WT mice as previously described¹⁸ and cultured in

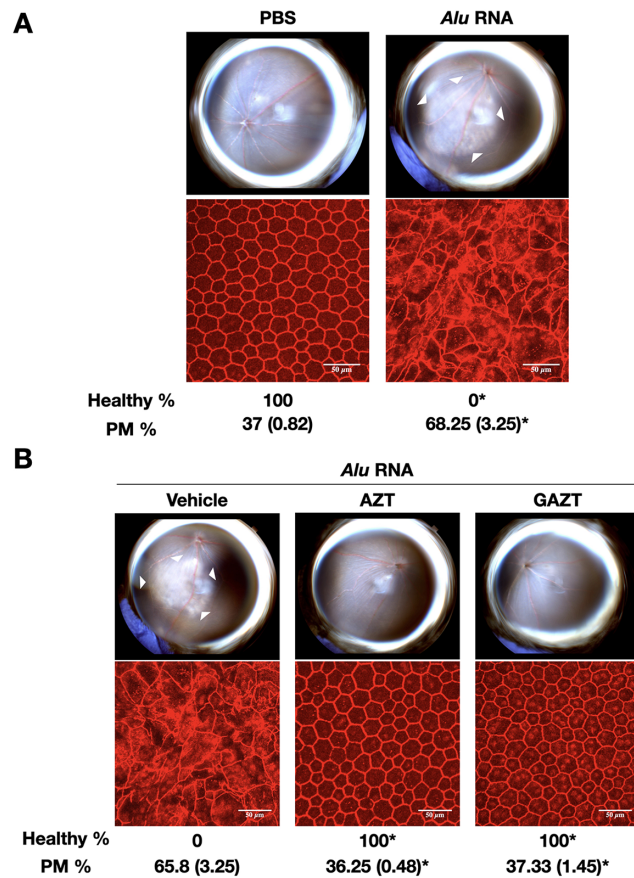


FIGURE 1. AZT and GAZT inhibit *Alu* RNA-induced RPE degeneration. Fundus photographs (*top row*) and RPE flat mounts stained for ZO-1 (*red, bottom row*) of mice injected subretinally with *Alu* RNA. RPE degeneration is outlined by *white arrowheads* in the fundus photographs. (A) Subretinal injection of *Alu* RNA induced RPE degeneration in WT mice ($n = 8$). (B) Intravitreal administration of AZT (0.5 nmol) and GAZT (0.5 nmol) blocked *Alu* RNA-induced RPE degeneration ($n = 12$). Binary (percent healthy) and morphometric (PM, polymegathism) quantification of RPE degeneration, mean (SEM), are shown (Fisher's exact test for binary; two-tailed *t*-test for morphometry; * $P < 0.001$). Loss of regular hexagonal cellular boundaries in ZO-1-stained flat mounts is indicative of degenerated RPE. Scale bars: 50 μ m.

Iscove's Modified Dulbecco's Medium (Thermo Fisher Scientific, Waltham, MA, USA) with 10% fetal bovine serum and 30% L929 supernatants, non-essential amino acids, sodium pyruvate, 2-mercaptoethanol, and antibiotics.

In Vitro Synthesis of *Alu* RNA

Alu RNA was synthesized using an in vitro transcription kit (AmpliScribe T7-Flash Transcription Kit; Epicentre, Madison, WI, USA) from a linearized plasmid containing a consensus *Alu* Y sequence with an adjacent T7 promoter following the manufacturer's instructions. The resulting *Alu* RNA was treated with DNase and purified (Invitrogen Ambion MEGAclear; Thermo Fisher Scientific), and integrity was monitored by gel electrophoresis.

Cell Transfection and Treatment

Overnight, in six-well cell culture dishes, 1.2 million cells/mL were seeded per well and pretreated with AZT or GAZT at

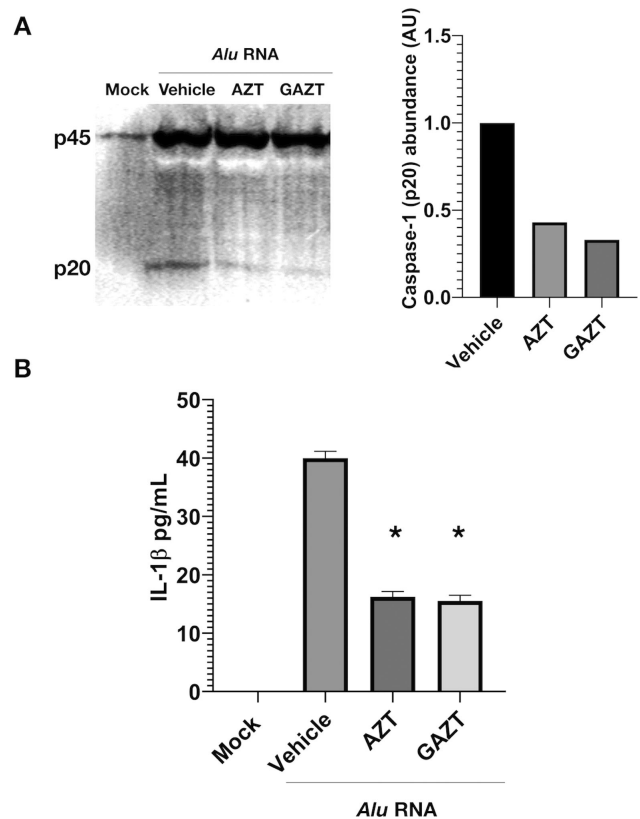


FIGURE 2. AZT and GAZT inhibit *Alu* RNA-induced inflammasome activation in cells. (A) Western blot of the caspase-1 pro (p45) and active (p20) forms in BMDMs transfected with *Alu* RNA and treated with PBS, AZT (200 μ M), or GAZT (200 μ M). Densitometric quantification of active caspase-1 (p20) bands in the immunoblot is shown in the bar graph. Representative blots ($n = 3$). (B) ELISA analysis of secreted IL-1 β in BMDMs mock-transfected or transfected with *Alu* RNA and treated with vehicle, AZT, or GAZT. * $P < 0.05$ (two-tailed *t*-test; $n = 3$; data are represented as mean \pm SEM).

200 μ M for 1 hour. Cells were transfected with *Alu* RNA overnight using Invitrogen Lipofectamine 3000 Transfection Reagent (Thermo Fisher Scientific) according to the manufacturer's instructions.

Western Blotting

Serum-free media (1 mL) from stimulated BMDMs were transferred into fresh tubes and centrifuged for 10 minutes at 12,000 rpm at 4°C; 15 μ L of 10% sodium deoxycholate was then added to the supernatants, vortexed, and kept on ice. Trichloroacetic acid (72 μ L; Sigma-Aldrich) was subsequently added, and the tubes were kept on ice overnight. After centrifugation for 30 minutes at 12,000 rpm at 4°C, the pellet was washed twice with 500 μ L ice-cold acetone. The pellet was dried and boiled with LDS Sample Buffer and β -mercaptoethanol (Sigma-Aldrich). The precipitated protein was resolved by 4% to 12% or by 4% to 20% Invitrogen Novex Tris-Glycine Gels (Thermo Fisher Scientific) and transferred onto Immun-Blot Low Fluorescence PVDF Membrane (1704274; Bio-Rad, Hercules, CA, USA). The transferred membranes were blocked with blocking buffer (927-40000; LI-COR, Lincoln, NE, USA) and incubated with anti-mouse caspase-1 (AG-20B-0042; AdipoGen Life Sciences, San Diego, CA, USA). The signal was visualized

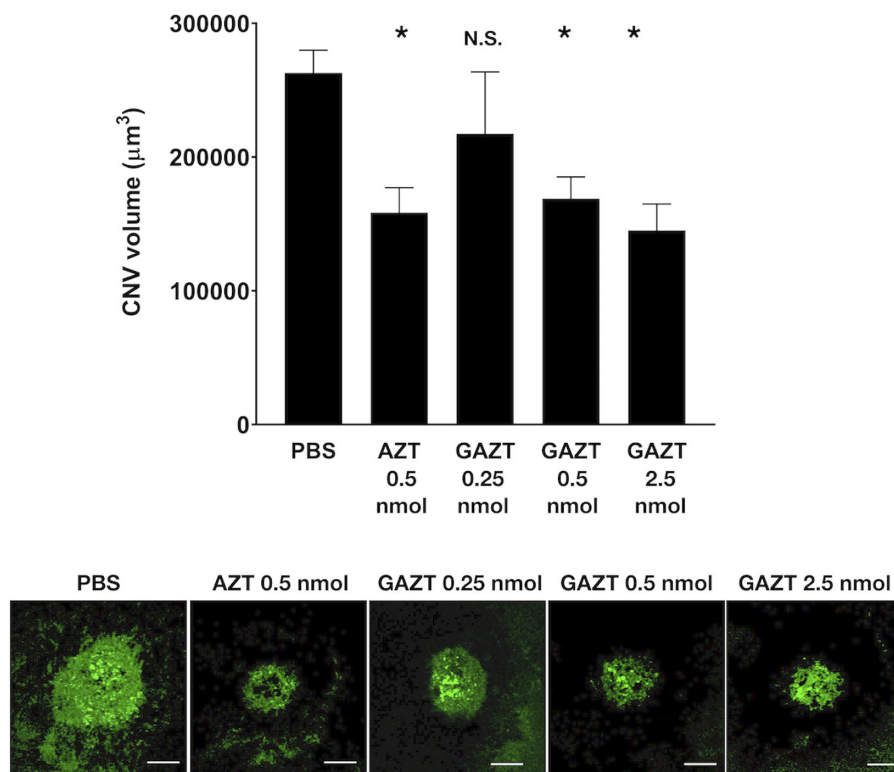


FIGURE 3. AZT and GAZT suppressed laser-induced CNV volume in WT mice. Intravitreal administration of AZT and GAZT significantly suppressed laser-induced CNV volume in WT mice in a dose-dependent manner. Data are means \pm SEM ($n = 8$ per group). $P < 0.05$ by one-way ANOVA with Bonferroni post hoc test. N.S., not significant. *Bottom:* Representative images of FITC-isolectin CNV lesions in RPE-choroid flat mounts. *Scale bars:* 100 μ m.

with secondary antibodies conjugated with IRDye and the Odyssey CLx Imaging System (LI-COR).

ELISA

Overnight, in six-well cell culture dishes, 1.2 million cells/mL were seeded per well and stimulated as mentioned above. Secreted mouse IL-1 β in the medium was detected by ELISA (Mouse IL-1beta/IL-1F2 DuoSet, DY401; R&D Systems, Minneapolis, MN, USA) according to the manufacturer's instructions.

Statistics

ELISA data are expressed as mean \pm SEM and were analyzed using Student's *t*-test. CNV volume results are expressed as mean \pm SEM ($n =$ number of eyes), with $P < 0.05$ considered statistically significant as determined by one-way ANOVA. Post hoc comparison of means was performed with a Bonferroni adjustment for multiple comparisons.

RESULTS

GAZT Blocks *Alu* RNA-Induced RPE Degeneration

We have previously demonstrated that *Alu* RNA accumulates in the RPE in GA, and subretinal injection of *Alu* RNA induces RPE degeneration in WT mice.¹⁷ Here, we examined whether GAZT blocks *Alu* RNA-induced RPE degeneration. Subretinal injection of *Alu* RNA induced RPE degeneration in

WT mice (Fig. 1A). Intravitreal administration of AZT and GAZT blocked *Alu* RNA-induced RPE degeneration (Fig. 1B).

GAZT Inhibits *Alu* RNA-Induced Inflammasome Activation

Next, we investigated the efficacy of GAZT by testing its ability to inhibit the NLR family pyrin domain containing 3 (NLRP3) inflammasome activation, a critical mediator of *Alu* RNA-induced cytotoxicity.¹⁵ Macrophages have been previously reported to have a role in the pathogenesis of both GA and CNV.^{19–21} Additionally, as *Alu* RNA-induced inflammasome signaling is similar in both BMDMs and RPE, we used BMDMs to study the effect of GAZT on *Alu* RNA-induced inflammasome activation.¹⁶ *Alu* RNA transfection induced caspase-1 activation and cleavage in BMDMs, and both AZT and GAZT inhibited *Alu* RNA-induced caspase-1 activation (Fig. 2A). *Alu* RNA transfection induced increased release of IL-1 β , and both AZT and GAZT inhibited this *Alu* RNA-induced IL-1 β release (Fig. 2B).

GAZT Suppresses Laser-Induced CNV

In addition to their anti-inflammatory activity, NRTIs also exhibit anti-angiogenic activity and suppress laser-induced CNV.⁸ Hence, we investigated whether GAZT treatment affects laser-induced CNV. Intravitreal administration of AZT and GAZT suppressed laser-induced CNV volume in WT mice in a dose-dependent manner (Fig. 3).

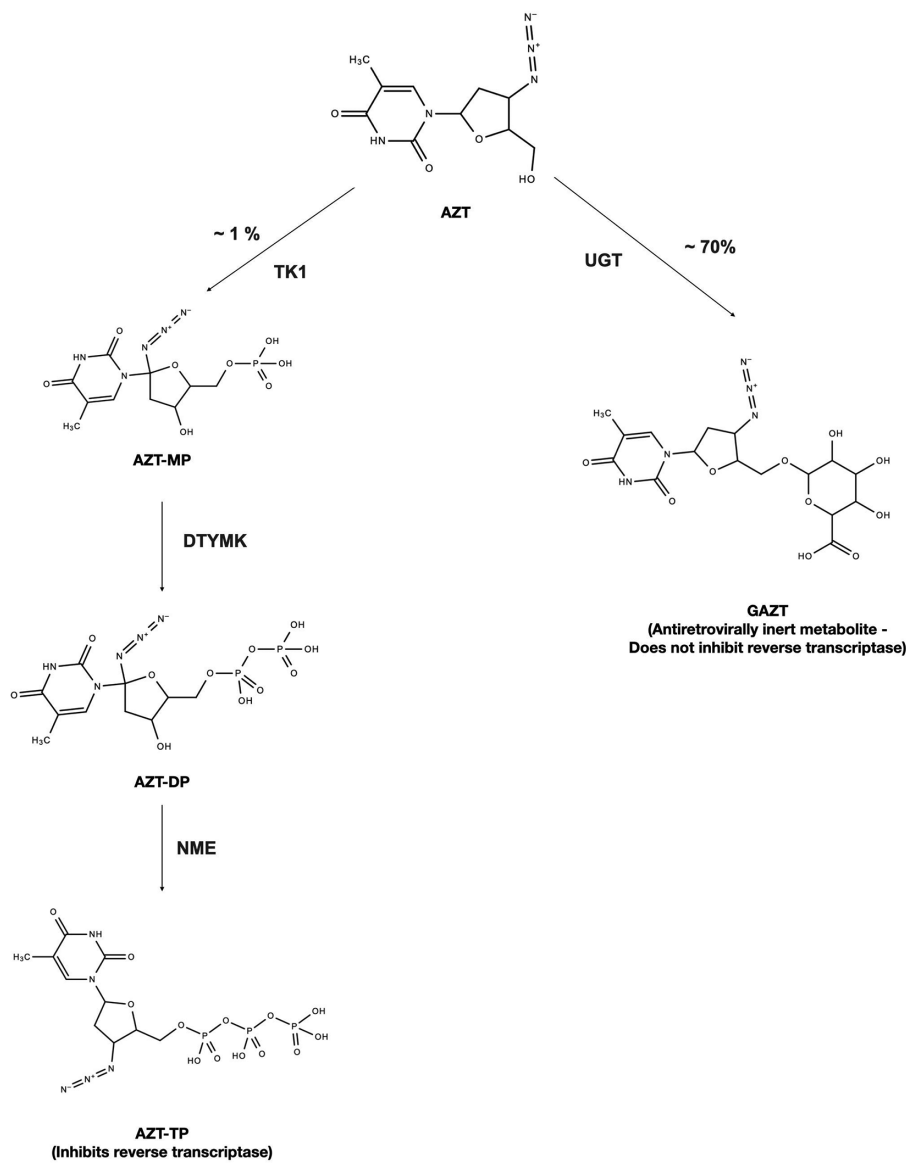


FIGURE 4. Structure and metabolism of AZT. AZT-MP, azidothymidine monophosphate; AZT-DP, azidothymidine diphosphate; AZT-TP, azidothymidine triphosphate; DTYMK, deoxythymidylate kinase; NME, nucleoside diphosphate kinase; TK1, tyrosine kinase 1; UGT, uridine 5'-diphospho-glucuronosyltransferase.

DISCUSSION

The present study not only reiterates the anti-inflammatory and anti-angiogenic properties of NRTIs but also identifies and demonstrates the efficacy of GAZT, a relatively non-toxic clinical metabolite of AZT, in mouse models of RPE degeneration and CNV. Additionally, we also observed that the anti-inflammatory and anti-angiogenic potency of GAZT was similar to its parent compound, AZT, at equimolar concentrations.

Despite continuing advances in our understanding of AMD, translation of this knowledge into safe and efficacious therapeutic strategies remains a persistent challenge, particularly for atrophic AMD. The time-consuming process of new drug development, escalating costs, and changing regulatory requirements are largely responsible for this challenge. Drug repurposing is an efficient drug development strategy to identify novel functions and uses for approved or inves-

tigational drugs that are outside the scope of the original medical indication.²²

As their name implies, NRTIs inhibit retroviral replication by inhibiting HIV-1 reverse transcriptase (a viral DNA polymerase).²³ NRTIs such as AZT also inhibit the purinergic P2X7 receptor independent of their ability to inhibit reverse transcriptase.⁷ Inhibition of P2X7 proffers anti-inflammatory and anti-angiogenic activity to NRTIs, thus making them putative candidates to be repurposed for AMD treatment. However, the toxicity associated with systemic AZT usage reduces its suitability for repurposing.⁹ These toxicities arise from virus-versus-host polymerase selectivity, as NRTIs also act as substrates for host cell DNA polymerases.¹⁰⁻¹²

AZT is a pro-drug that requires phosphorylation at its 5' position by host kinases to transform into the antiretrovirally active triphosphate form (AZT-TP) (Fig. 4).²⁴ Chemical modifications of AZT at this 5' position prevent phosphorylation and thus also prevent the inhibition of reverse

transcriptase and host cell polymerases. Alkoxy modifications of AZT and other NRTIs, known as Kamuvudines, retain their anti-inflammatory properties despite lacking the ability to inhibit reverse transcriptase and thereby lacking the associated side effects.⁷ In spite of this exciting discovery, these synthetic NRTI derivatives would still be subject to certain regulatory requirements.

The predominant pathway of AZT metabolism in humans is uridine 5'-diphospho (UDP)-glucuronosyltransferase-mediated glucuronidation at its 5' position resulting in the formation of GAZT (Fig. 4).¹³ Akin to alkoxy modifications, this glucuronidation at the 5' site renders GAZT immune to host cell phosphorylation and incapable of incorporation into (and becoming inactive against) viral reverse transcriptase and host cell polymerases; hence, GAZT also would lack the attendant toxicities.^{13,14} Importantly, because GAZT comprises >10% of total AZT-related exposure (~70%), it would be expected, per US Food and Drug Administration regulations to qualify for human use as a disproportionate drug metabolite.²⁵ The collective experimental data and established safety profile highlight the translational potential of GAZT and potentially other anti-retrovirally inert modified NRTIs for the treatment of AMD. Our study shows that GAZT retains the anti-inflammatory and anti-angiogenic activity of AZT and provides impetus to consider GAZT as a safe and viable drug candidate ripe for clinical studies in both forms of AMD.

Acknowledgments

Supported by National Institutes of Health grants (R01EY028027, R01EY029799), the DuPont Guerry III Professorship, and the University of Virginia Strategic Investment Fund. BDG is supported by National Institutes of Health grant R01EY029799. No funding agency had a role in study design or conduct, data collection, analysis, interpretation, or manuscript writing. The content of this article is solely the responsibility of the authors and does not necessarily represent the official views of the National Institutes of Health nor does mention of trade names, commercial products, or organizations imply endorsement by the US Government.

Disclosure: **S. Narendran**, University of Virginia (P); **F. Pereira**, University of Virginia (P); **P. Yerramothu**, None; **I. Apicella**, University of Virginia (P); **S.-B. Wang**, University of Virginia (P); **A. Varshney**, None; **K.L. Baker**, None; **K.M. Marion**, None; **M. Ambati**, University of Virginia (P); **V.L. Ambati**, None; **K. Ambati**, University of Virginia (P), University of Kentucky (P); **S.R. Sadda**, 4DMT (C), Allergan (C), Amgen (C), Carl Zeiss Meditec (F), Centervue (C), Heidelberg Engineering (C), Roche/Genentech (C), Novartis (C), Optos (C), Regeneron (C), Oxurion (C), Merck (C), Topcon (F), Nidek (F); **B.D. Gelfand**, University of Virginia (P); **J. Ambati**, iVeena Holdings (S), iVeena Delivery Systems (S), Inflammasome Therapeutics (P, S), Allergan (C, R), Immunovant (C), Olix Pharmaceuticals (C), Saksin LifeSciences (C, R), University of Virginia (P), University of Kentucky (P)

References

- Wong WL, Su X, Li X, et al. Global prevalence of age-related macular degeneration and disease burden projection for 2020 and 2040: A systematic review and meta-analysis. *Lancet Glob Health*. 2014;2:e106–e116.
- Wright CB, Uehara H, Kim Y, et al. Chronic Dicer1 deficiency promotes atrophic and neovascular outer retinal

- pathologies in mice. *Proc Natl Acad Sci USA*. 2020;117:2579–2587.
- Sarks SH. Ageing and degeneration in the macular region: a clinico-pathological study. *Br J Ophthalmol*. 1976;60:324–341.
- Sunness JS, Gonzalez-Baron J, Bressler NM, Hawkins B, Applegate CA. The development of choroidal neovascularization in eyes with the geographic atrophy form of age-related macular degeneration. *Ophthalmology*. 1999;106:910–919.
- Sadda SVR, Tuomi LL, Ding B, Fung AE, Hopkins JJ. Macular atrophy in the HARBOR study for neovascular age-related macular degeneration. *Ophthalmology*. 2018;125:878–886.
- Ambati J, Fowler BJ. Mechanisms of age-related macular degeneration. *Neuron*. 2012;75:26–39.
- Fowler BJ, Gelfand BD, Kim Y, et al. Nucleoside reverse transcriptase inhibitors possess intrinsic anti-inflammatory activity. *Science*. 2014;346:1000–1003.
- Mizutani T, Fowler BJ, Kim Y, et al. Nucleoside reverse transcriptase inhibitors suppress laser-induced choroidal neovascularization in mice. *Invest Ophthalmol Vis Sci*. 2015;56:7122–7129.
- Rachlis A, Fanning MM. Zidovudine toxicity. Clinical features and management. *Drug Saf*. 1993;8:312–320.
- Cooper DL, Lovett ST. Toxicity and tolerance mechanisms for azidothymidine, a replication gap-promoting agent, in *Escherichia coli*. *DNA Repair (Amst)*. 2011;10:260–270.
- Mislak AC, Anderson KS. Insights into the molecular mechanism of polymerization and nucleoside reverse transcriptase inhibitor incorporation by human PrimPol. *Antimicrob Agents Chemother*. 2016;60:561–569.
- Johnson AA, Ray AS, Hanes J, et al. Toxicity of antiviral nucleoside analogs and the human mitochondrial DNA polymerase. *J Biol Chem*. 2001;276:40847–40857.
- Veal GJ, Back DJ. Metabolism of zidovudine. *Gen Pharmacol*. 1995;26:1469–1475.
- Moore KH, Raasch RH, Brouwer KL, et al. Pharmacokinetics and bioavailability of zidovudine and its glucuronidated metabolite in patients with human immunodeficiency virus infection and hepatic disease (AIDS Clinical Trials Group protocol 062). *Antimicrob Agents Chemother*. 1995;39:2732–2737.
- Tarallo V, Hirano Y, Gelfand BD, et al. DICER1 loss and Alu RNA induce age-related macular degeneration via the NLRP3 inflammasome and MyD88. *Cell*. 2012;149:847–859.
- Kerur N, Fukuda S, Banerjee D, et al. CGAS drives noncanonical-inflammasome activation in age-related macular degeneration. *Nat Med*. 2018;24:50–61.
- Kaneko H, Dridi S, Tarallo V, et al. DICER1 deficit induces Alu RNA toxicity in age-related macular degeneration. *Nature*. 2011;471:325–332.
- Zhang X, Goncalves R, Mosser DM. The isolation and characterization of murine macrophages. *Curr Protoc Immunol*. 2008;83:14.1.1–14.1.14.
- McLeod DS, Bhutto I, Edwards MM, Silver RE, Seddon JM, Luttj GA. Distribution and quantification of choroidal macrophages in human eyes with age-related macular degeneration. *Invest Ophthalmol Vis Sci*. 2016;57:5843–5855.
- Sakurai E, Anand A, Ambati BK, van Rooijen N, Ambati J. Macrophage depletion inhibits experimental choroidal neovascularization. *Invest Ophthalmol Vis Sci*. 2003;44:3578–3585.
- Grossniklaus HE, Cingle KA, Yoon YD, Ketkar N, L'Hernault N, Brown S. Correlation of histologic 2-dimensional reconstruction and confocal scanning laser microscopic imaging of choroidal neovascularization in eyes with

- age-related maculopathy. *Arch Ophthalmol*. 2000;118:625–629.
22. Pushpakom S, Iorio F, Eyers PA, et al. Drug repurposing: progress, challenges and recommendations. *Nat Rev Drug Discov*. 2018;18:41–58.
 23. Holec AD, Mandal S, Prathipati PK, Destache CJ. Nucleotide reverse transcriptase inhibitors: a thorough review, present status and future perspective as HIV therapeutics. *Curr HIV Res*. 2017;15:411–421.
 24. Furman PA, Barry DW. Spectrum of antiviral activity and mechanism of action of zidovudine. An overview. *Am J Med*. 1988;85:176–181.
 25. US Department of Health and Human Services, Food and Drug Administration, Center for Drug Evaluation and Research (CDER). Safety testing of drug metabolites: guidance for industry. Available at: <https://www.fda.gov/media/72279/download>. Accessed July 27, 2020.